Evidence for an α-Helix → π-Bulge Helicity Modulation for the *neu*/*erbB-2* Membrane-Spanning Segment. A ^{1}H NMR and Circular Dichroism Study[†,‡]

Michael Goetz,[§] Claire Carlotti,[§] François Bontems,[||] and Erick J. Dufourc*[,§]

Institut Européen de Chimie et de Biologie, Ecole Polytechnique, CNRS & Universités de Bordeaux I et II, Talence, France, and DCSO, Ecole Polytechnique, CNRS, Palaiseau, France

Received December 8, 2000; Revised Manuscript Received February 16, 2001

ABSTRACT: The 35-residue peptide corresponding to the very hydrophobic transmembrane region of the tyrosine kinase receptor *neu*, Neu$_{TM35}$, has been synthesized. The peptide can be solubilized in millimolar concentrations in TFE or incorporated into an SDS−water micellar solution or into well-hydrated DMPC/DCPC bicelles. In all these media, circular dichroism demonstrated that the peptide adopts a helical structure for about 80% of its amino acids. The peptide is monomeric below 2 mM in TFE, as also determined by variable concentration experiments. The three-dimensional solution structure in TFE has been obtained by homonuclear proton NMR and shows a well-defined α-helix from residues 4 to 21, then a π-bulge from Ile^{22} to Gly^{28}, and a final short α-helix from positions 29 to 32. This experimental finding is in agreement with structures predicted recently by molecular dynamics calculations in a vacuum [Sajot, N., and Genest, M. (2000) *Eur. Biophys. J. 28*, 648−662]. The biological implications of a possible retention of this structure in a membrane environment are finally discussed.

Growth factor receptors of the tyrosine kinase family consist of two large, separately folded domains, one external and one cytosolic, connected by a single transmembrane segment. The sequence of the membrane-spanning peptide appears to be important for function. For example, a single point mutation in the proto-oncogene *neu*, resulting in a substitution of a valine residue for glutamic acid at position 664 within the transmembrane region, may transform it into an oncogene (*1*−*3*). The mutant receptor then has constitutive tyrosine kinase activity in the absence of ligand, apparently as a result of greatly enhanced receptor dimerization (*4*).

The hypothesis of a key role played by the single transmembrane domain in the dimerization process has also been put forward for other membrane proteins such as the insulin receptor (*5*) or the fibroblast growth factor (*6*). Activating mutation has been suggested to act as a stabilizer of the transmembrane helix structure, which would favor inter-receptor packing (*7*). This packing could be enhanced by hydrogen bonding interactions promoted by the mutated amino acid, as proposed by Smith and co-workers for neu TM[1] helices embedded in lipid bilayers (*3*). Alternatively, modulation of the TM helicity by π local defects termed 'π-bulges' could also favor inter-helix hydrogen bond interactions (*8*). In a recent study, Genest and co-workers (*9*) predicted from molecular dynamics simulations that these defects would be present and could modulate the helicity of neu/ErbB-2 transmembrane domains.

Only very few membrane-bound proteins have had their three-dimensional structure resolved at an atomic scale to this day, contrary to the tens of thousands of hydrosoluble proteins. This is mainly due to enormous difficulties in production, purification, and crystallization inherent to their hydrophobic character. In the case of *neu/erbB-2*, the membrane-embedded domain consists of a sequence of approximately 30 residues, harboring the critical spot of oncogenic mutation. The only attempt, to our knowledge, of high-resolution structure of the neu protein transmembrane segment has been obtained by replacing some hydrophobic amino acids by serine in the synthesis of a 18-residue peptide. This improved peptide solubility and facilitated purification and analysis (*10*). We decided to realize by means of adapted solid-phase synthesis the 35-residue transmembrane peptide Neu$_{TM35}$ corresponding to residues 650−684 of the full-length native receptor. In the present work, the peptide will be numbered 1−35; the point mutation that may occur at Val^{664} will then correspond to Val^{15} in our sequence. In this paper, we describe the structural investigation of this peptide both by NMR spectroscopy in TFE and by circular dichroism

[†] This work is supported by grants from the Ecole Polytechnique and the Region Aquitaine.

[‡] Coordinates of *neu* membrane segment Neu$_{TM35}$ have been deposited in the PDB under accession number 1IIJ. Chemical shifts are available as Supporting Information.

* Address correspondence to this author at IECB-Polytechnique, FRE CNRS 2247, 16 Av. Pey-Berland, 33607 Pessac Cedex, France. Tel+Fax: +33557962218; email: erick.dufourc@iecb-polytechnique.u-bordeaux.fr.

[§] Institut Européen de Chimie et de Biologie, Ecole Polytechnique.

[||] DCSO, Ecole Polytechnique.

[1] Abbreviations: 2D NMR, two-dimensional nuclear magnetic resonance; TFE, trifluoroethanol; DMPC, dimyristoylphosphatidylcholine; DCPC, dicaproylphosphatidylcholine; HPLC, high-performance liquid chromatography; SDS, sodium dodecyl sulfate; DMSO, dimethyl sulfoxide; TFA, trifluoroacetic acid; CD, circular dichroism; DQF-COSY, double-quantum-filtered correlation spectroscopy; NOESY, nuclear Overhauser 2D spectroscopy; HOHAHA, homonuclear Hartman−Hahn 2D correlation spectroscopy; Neu$_{TM35}$, 35-residue peptide of the transmembrane region of the *neu* tyrosine kinase receptor; TM, transmembrane; RMSD, root-mean-square deviation.

10.1021/bi0027938 CCC: $20.00
Published on Web 05/03/2001

while embedded in various media such as detergent micelles or bicellar phospholipid model membranes. This is the first step toward comprehension of the relation between structure, dimer formation, tyrosine kinase activation, and cell transformation. As will be shown below, the peptide is mainly α-helical in TFE solution, micelles, and membranes, and the structure as found from NMR contains a well-located short π-bulge within the α-helix.

MATERIALS AND METHODS

Chemicals. Amino acids and resin for solid-phase synthesis were purchased from Novabiochem (Läufelfingen, Switzerland). Solvents and reagents for synthesis and HPLC were of grade A and obtained from Sigma (St. Quentin, France). SDS and TFE were also purchased from Sigma (St. Quentin, France). DCPC and DMPC to form bicelles were purchased from Avanti Polar Lipids (Birmingham, AL). Deuterated TFE was obtained from Eurisotop (Saclay, France).

Peptide Synthesis and Purification. The chemical synthesis of the Neu_{TM35} peptide (^{650}EQRASPVTFIIATVV^{664}-GVLLFLILVVVVGILIKRRR^{684}) was performed on an Applied Biosystems Peptide Synthesizer 433A (PE Biosystems, Courtaboeuf, France) using the Fmoc strategy (*11, 12*) as outlined below for clarity. DMSO was added during difficult coupling steps to increase the coupling efficiency by helping to break self-aggregation of growing peptide hydrophobic chains. At the end of each coupling step, unreacted amine positions were acetylated. The final peptide mixture was cleaved from the resin by TFA treatment.

The lyophilized product was dissolved in a mixture of 75% acetonitrile in MilliQ-water, both containing 0.08% TFA, and loaded onto a Superdex Peptide HR 10/30 column (Amersham Pharmacia Biotech, Orsay, France) using an ÄKTA explorer 100 liquid chromatography system (Amersham Pharmacia Biotech, Orsay, France) for primary purification. A second chromatographic step was done on a Waters Alliance HPLC station using a Waters DeltaPak C_4 column (5 μm, 100 Å, 3.9 × 150 mm) (Waters S. A., St. Quentin, France). Separation conditions as well as mass spectrometric analyses, monitoring the synthetic peptides' high degree of purity, superior to 95%, are described in detail in (*11*). Peptide numbering in what follows will be 1−35, corresponding to 650−684 of the primary sequence.

Circular Dichroism. Circular dichroism (CD) spectra were run on a Mark VI Jobin Yvon dichrograph at 0.2 nm intervals over the wavelength range 184−270 nm. The dichrograph was calibrated using *iso*-androsterone (Roussel-Uclaf, France) in dioxane and camphorsulfonic acid in water. The optical rotation was checked with cytochrome *c* (horse heart) and calmodulin, lysozyme (chicken egg white), all from Sigma−Chimie (St. Quentin, France). Measurements were carried out at room temperature with 1 mm path length cells, in trifluoroethanol (TFE), in sodium dodecyl sulfate (SDS) micelles, and in DMPC/DCPC bicelles (1,2-dimyristoyl-/dicaproyl-*sn*-glycero-3-phosphocholine), at 35 °C. The mole content of DMPC was fixed to $x = 75\%$, with a total lipid hydration of 90% (v/v). This corresponds, at 35 °C, to the middle of the bicelle domain phase diagram as reported in (*13*). Peptide concentrations in the different media were as follows: TFE (600 μM), SDS (50 μM), bicelles (900 μM, peptide-to-lipid ratio 0.5 mol %). For the measurement of the $\Delta\epsilon_{220\ nm}/\Delta\epsilon_{208\ nm}$ ratio, we used a 1 mm path length cell for concentrations ranging from 10 to 200 μM and a 0.1 mm path length cell for concentrations ranging from 200 to 2000 μM Neu_{TM35} in TFE.

NMR Spectroscopy. The lyophilized synthetic peptide was dissolved in deuterated trifluoroethanol (TFE-d_2) to concentrations of 1.5 mM. The 2D NMR spectra were recorded at 27 °C on Bruker Advance DPX 400, DSX 500, and DRX 600 spectrometers. The OH resonance of TFE was suppressed by selective saturation during the relaxation delay. DQF-COSY, HOHAHA, and NOESY spectra were acquired in the phase-sensitive mode by time-proportional phase incrementation (TPPI) of the first pulse (*14*). The 90° pulse ranged from 5 to 6 μs; the spectral width was 9.5 ppm for the experiments reported here. HOHAHA spectra were recorded using the MLEV pulse scheme with 30, 60, 70, and 90 ms isotropic mixing periods. NOESY experiments were recorded with mixing times of 100 and 300 ms. The data sizes were usually 2048 complex points in the t_2 dimension and 512 (NOESY) or 496 (HOHAHA and COSY) t_1 increments. A total of 176 scans were acquired for the HOHAHA and COSY experiments, and 112 scans for the NOESY experiments. GIFA software was used to process the NMR data (*15, 16*). After zero-filling to 2K in both dimensions, the two-dimensional data matrixes were multiplied by a shifted sine-bell window function (em = −5, gm = 10, sin = 0.2) and Fourier-transformed (*14*). Distance constraints were obtained from cross-peak intensities of NOESY experiments, as determined with the XEASY package (*17*). Whenever the assignment of distance constraints to an atom pair was not stereospecific, pseudoatoms were introduced and distance corrections added. Preliminary structure calculations were performed with the aid of the program DYANA (*18*), following standard protocols.

Molecular Mechanics. Calculations were performed on a R10000 SGI workstation running InsightII and Discover ver. 97.0 (Molecular Simulations Inc.) with the CVFF force field. The DYANA output files (PDB format) were used as input files within Discover, and a 12 Å group-based cutoff was used throughout the calculations. All side chains and terminations were uncharged. In the first step, all systems were minimized with the protein backbone fixed using 300 conjugate gradient (CG) steps, then the backbone was tethered using a constraint which was lowered in a stepwise manner (100/300 CG, 50/300 CG, and 25/500 CG), and finally minimization was resumed unconstrained using CG until the RMS was between 10^{-2} and 10^{-3}.

RESULTS

CD Spectroscopy. The synthetic 35-residue peptide is composed of almost 70% nonpolar amino acids. Only amphiphilic or organic solvents, like TFE or DMSO, solubilized efficiently this hydrophobic product. To identify ideal conditions for NMR analysis and determine to a crude degree the overall secondary structure of this peptide, we performed circular dichroism spectroscopy. Figure 1 shows the spectral superimposition of Neu_{TM35} peptide in TFE, in 500 μM SDS (micellar conditions), and in 90% hydrated DMPC/DCPC bicelles. Although there are differences in the three curves, all show pronounced positive (190 nm) and

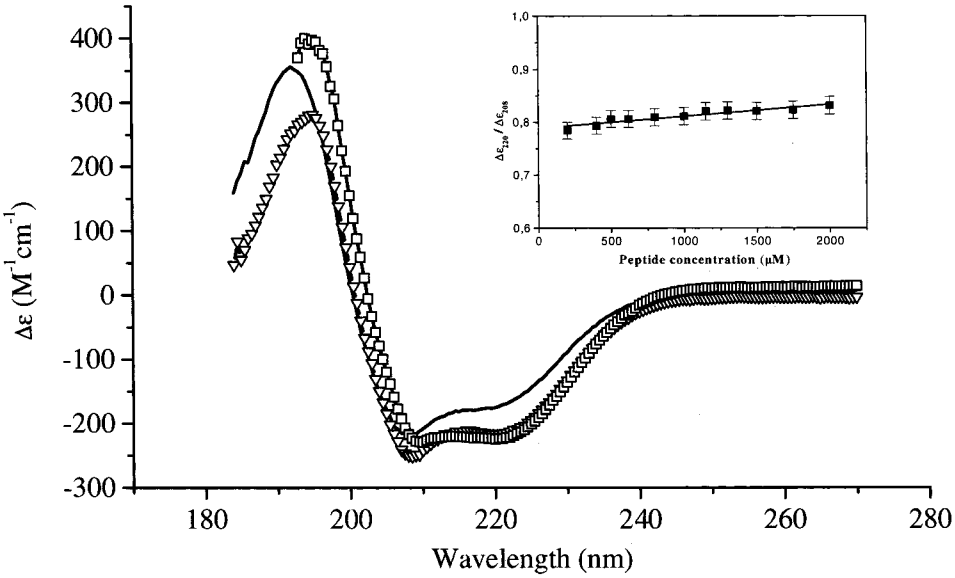

FIGURE 1: Circular dichroism spectra of the Neu_{TM35} peptide in TFE (620 μM, solid line), in 500 mM SDS micelles (50 μM, triangles), and in DMPC/DCPC bicelles (900 μM, squares). Spectra were recorded at either room temperature (TFE, SDS) or 35 °C (bicelles). The inset shows the $\Delta\epsilon_{220\ nm}/\Delta\epsilon_{208\ nm}$ linearity at peptide concentrations between 200 and 2000 μM in TFE.

negative (208, 220 nm) absorption bands. Commonly used deconvolution algorithms propose an over 80% α-helical contribution to the overall content of the peptides' secondary structural elements (*19*). Although the algorithms tend to show that there is more helix content in SDS and membrane media than in TFE, the figures are within the intrinsic inaccuracy of the methods, so we only quote 80%. It should also be pointed out that experiments performed with the peptide dissolved in TFE, in the presence of increasing amounts of subsequently added water (not shown), did not bring noticeable spectral differences.

In NMR experiments, sensitivity increases the higher the concentration of the protein sample. The limiting factor being aggregation, we looked at possible peptide oligomerization by studying the influence of peptide concentration on the helix content. In CD spectroscopy, the ratio $\Delta\epsilon_{220\ nm}/\Delta\epsilon_{208\ nm}$ is widely used to assess whether α-helices are implicated in coiled-coil motifs, the translation of homodimer formation (*20*). A $\Delta\epsilon_{220\ nm}/\Delta\epsilon_{208\ nm}$ ratio of about 0.8 is proposed for a single-stranded helix and of about 1.0 for a two-stranded α-helical coiled-coil (*21, 22*). The inset in Figure 1 shows the values of $\Delta\epsilon_{220\ nm}/\Delta\epsilon_{208\ nm}$ for *neu* peptide concentrations ranging from 20 to 2000 μM. A slight slope is noticed, suggesting traces of aggregation, but within these limits, the ratio stays close to a mean value of 0.81, indicating mostly the absence of dimerization phenomena. The presence of dimeric species in this concentration range would have been characterized by a "first order" like transition as has been reported for other peptides or proteins (*20*).

NMR Analysis and Structure Calculation. We recorded homonuclear proton 2D spectra at peptide concentrations of 1.5 mM. The cross-peak assignment was performed according to the procedure proposed by Wüthrich (*23*). Spin systems were identified by HOHAHA and DQF-COSY experiments (spectra not shown), and connected by virtue of sequential $d_{\alpha N}$, d_{NN}, and/or $d_{\beta N}$ connectivities, detected on the NOESY spectra represented in Figures 2−4. The sequential $H\alpha_{(i)}-HN_{(i+1)}$ and $HN_{(i)}-HN_{(i+1)}$ pathways are drawn on the fingerprint (Figure 3) and the amide regions (Figure 4), respectively. This strategy led to complete proton assignment (proton resonances are listed in Table 1 that is available as Supporting Information). The non-random-coil behavior of the Neu_{TM35} peptide, as suggested by CD studies, is confirmed by the presence of many medium-range connectivities throughout the sequence as summarized in Figure 5. Strong $HN_{(i)}-HN_{(i+1)}$ and $H\beta_{(i)}-HN_{(i+1)}$ as well as medium-range $HN_{(i)}-HN_{(i+2)}$, $H\alpha_{(i)}-H\beta_{(i+3)}$, $H\alpha_{(i)}-HN_{(i+3)}$, and $H\alpha_{(i)}-HN_{(i+4)}$ connectivities are characteristic of an α-helix. Interestingly, in the sequence spanning residues $Ile^{22}-Gly^{28}$, we observed essentially $H\alpha_{(i)}-HN_{(i+4)}$ plus a few $H\alpha_{(i)}-HN_{(i+5)}$ connectivities [see, for instance, $H\alpha(I^{22})-HN(V^{27})$ in Figure 3], suggesting local deformation of the regular α-helix.

NOESY cross-peak volumes were determined with the integration routines of XEASY (*17*) and related to upper distance limits (confined to the range 2.4−5.5 Å) with the module CALIBA within the program package DYANA. A total of 385 significant upper distance constraints were established; 111 dihedral angle constraints for the input in DYANA calculations were obtained using the module HABAS for a combined interpretation of the backbone−backbone intraresidual and sequential NOE upper distance limits, together with the measurable $^3J_{H\alpha-HN}$ and $^3J_{H\alpha-H\beta}$ coupling constants. HABAS also provided 16 stereospecific assignments for β- and γ-methylene protons. Structure calculations were performed using the anneal protocol within DYANA. Starting from 1000 initial structures with randomly chosen dihedral angles, we finally retained the best 12 conformers giving the lowest target−function values and satisfying the NOE distance and dihedral angle constraints nearly perfectly (no violation greater than 0.2 Å or 5°). The Neu_{TM35} peptide adopts an entirely helical conformation throughout the sequence. In the region between residues Ile^{22} and Gly^{28}, the α-helix experiences a local distortion identified by a series of "*i*, *i*+5" hydrogen bonds, resulting in a π-bulge spanning approximately two turns. We applied very careful molecular mechanics in order to minimize the peptide's overall energy, until the RMS deviation went below 0.01,

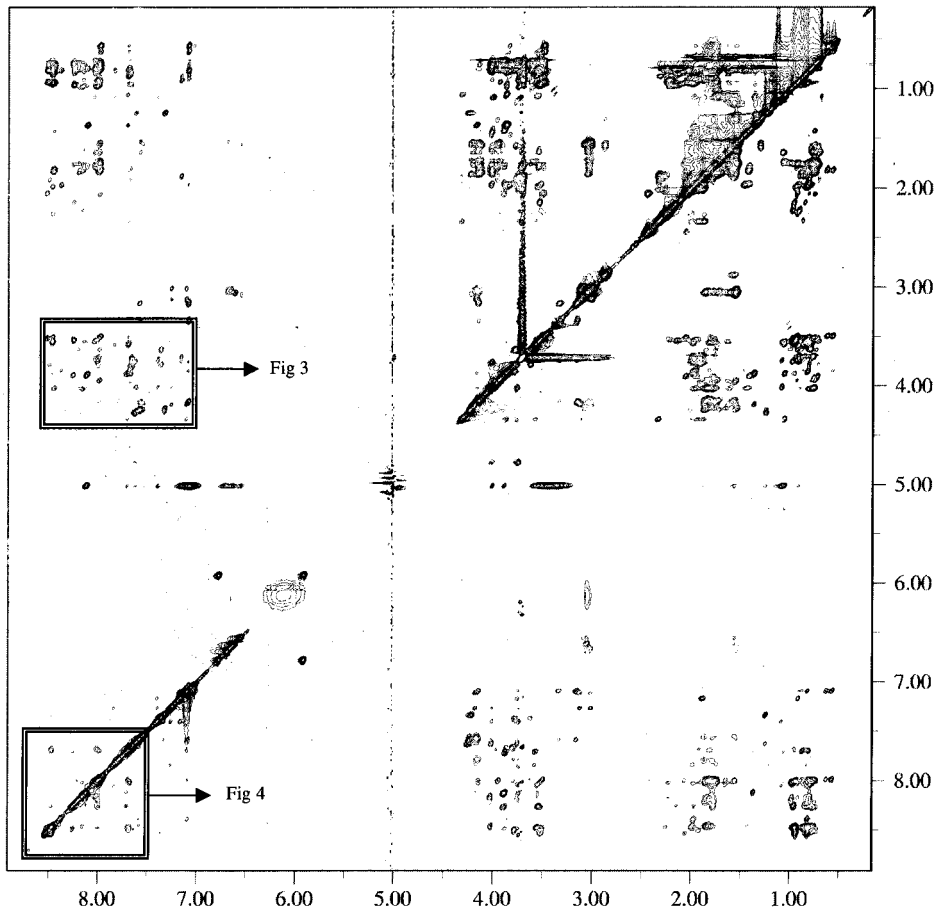

FIGURE 2: Contour plot of the NOESY spectrum recorded at 600 MHz, with 300 ms mixing time at 27 °C in 100% TFE. Highlighted areas are expanded in Figures 3 and 4.

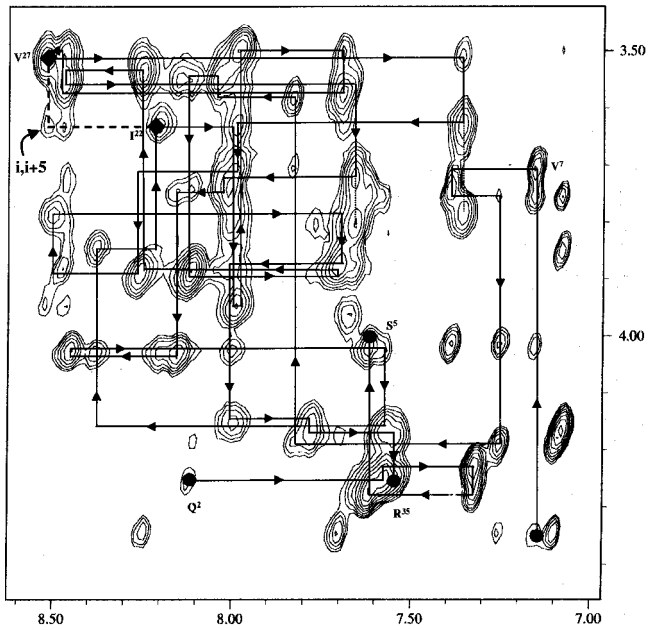

FIGURE 3: Expansion of the NOESY spectrum in the HN−Hα region, showing the sequential assignment. $HN_{(i)}-H\alpha_{(i)}-HN_{(i+1)}$ connections are drawn from Glu^2 to Ser^5 and from Val^7 to Arg^{35}. For clarity, only residues at both ends of the sequential assignment are labeled (filled circles). The medium-range ($i,i+5$) correlation of $H\alpha(Ile^{22})$ and $HN(Val^{27})$ is highlighted (filled diamonds connected by dashed lines).

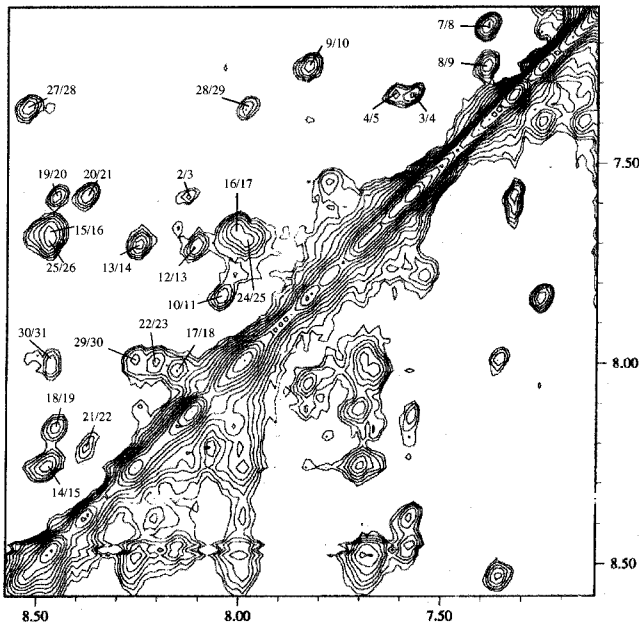

FIGURE 4: Expanded region of the NOESY spectrum, illustrating the cross-peaks between $NH_{(i)}$ and $NH_{(i+1)}$.

and finally retained the five best results. Figure 6 shows their superposition, best-fitted on residues 7−32. The Neu_{TM35} peptide's overall structure is well-defined with an RMS deviation for the backbone atoms of less than 0.96 Å. The molecule adopts an α-helix structure between positions 4 and 22. An π-helix is observed between positions 22 and 28; then a small part of α-helix reappears from positions 29 to 32.

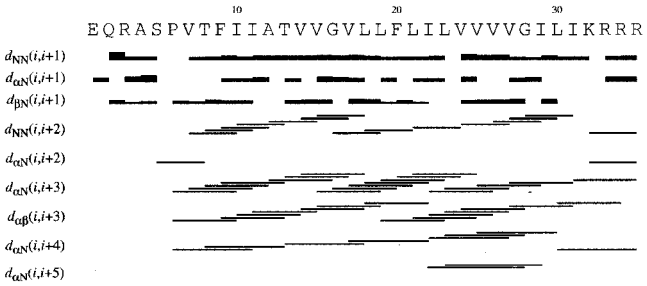

FIGURE 5: Summary of sequential and medium-range NOEs. Sequential NOEs are indicated with boxes whose sizes are proportional to the upper distance bound calculated from NOE intensity. The plot has been realized with the aid of the XEASY program (*14*).

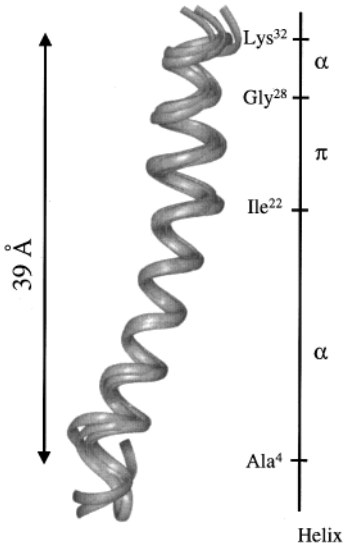

FIGURE 6: Superimposition of five energy-minimized structures (ribbon trace of the backbone) of the Neu_{TM35} peptide; the N-terminus is on top. Structures are best-fitted on residues 7−32, with an RMSD deviation for the backbone atoms of 0.96 Å. On the right-hand side of the figure, α- and π-helical regions are indicated as defined in the text.

DISCUSSION

In this work, three main results appear: (i) the synthesis and purification of the 35 aa very hydrophobic peptide *neu*, (ii) its solution structure by NMR, and (iii) the retention of the secondary structure in micelles and in phospholipid model membranes. These different points will be discussed below, with the possible biological implications of the finding of an $\alpha-\pi$ helicity modulation.

To perform NMR structure analysis, large quantities of highly pure protein are requested. For the production of the *neu* transmembrane segment ($Glu^{650}-Arg^{684}$), we decided to perform chemical synthesis, as the segment's shortness as well as its membranous location would make it difficult to realize by classic molecular biology techniques. Even with the well-established solid-phase method, membrane protein synthesis is far from being routine. Hydrophobic interactions are expected to induce strong intra- and interchain associations within the peptide-resin matrix, affecting reaction rates and lowering coupling yields. Early approaches to synthesize the hydrophobic *neu* segment have already been performed by making use of two general strategies: (i) making shorter peptides and replacing some hydrophobic residues by the polar residue serine in order to improve solubility (*10*); and (ii) synthesis of longer peptides with enough polar and charged amino acids on each side of the hydrophobic segment to counterbalance its large hydrophobic effect (*3*, *24*). Because the reaction yield is inversely proportional to peptide length, we remained, in our approach, as close as possible to the TM-spanning segment by synthesizing a 35 aa peptide with the potential mutagenic site at position 15, well in the middle of the sequence. We nevertheless modified the solid-phase synthesis protocol and especially adapted it to hydrophobic proteins. Orthogonal protein purification, based on gel-permeation and reverse-phase liquid chromatography, coupled to electrospray mass spectrometry, allowed us to obtain 10−21 mg amounts of highly pure product [results not shown; for more details, see (*11*, *12*)].

Membrane proteins require an amphiphilic environment for their proper folding and function. The adequate environment is of course the phospholipid membrane. As will be discussed later, Neu_{TM35} can indeed be inserted in a phospholipid membrane. However, it is much easier to perform 2D NMR experiments in an isotropic medium to obtain the 3D structure of the peptide. This is why we choose trifluoroethanol for peptide solubilization and subsequent spectroscopic analyses. CD spectra of the Neu_{TM35} peptide in pure TFE or in TFE−water media are in favor of pronounced α-helical content in a way very similar to what is obtained when it is embedded in membranes. This strongly suggests that the peptide has relevant folding in TFE. Because circular dichroism data suggest the existence of monomeric species in this solvent, to peptide concentrations up to 2 mM, we have elucidated the 3D structure of 1.5 mM Neu_{TM35} in deuterated TFE by means of homonuclear ^1H NMR spectroscopy. Spectral data obtained in HOHAHA, DQF-COSY, and NOESY experiments are consistent with the preliminary CD results. Based on large sets of short- and medium-range conformational constraints, we established a molecular model, where we observed an entirely helical conformation throughout the peptide core (Figure 5). NMR experimental data already suggested an α-helix distortion in the region Ile^{22}-Leu^{23}-Val^{24}-Val^{25}-Val^{26}-Val^{27}-Gly^{28}, which we confirmed by simulated annealing computational analysis. After careful minimization, we still observed "*i*, *i*+5" hydrogen bonds in this particular region, corresponding to a looser π-bulge that interrupts the α-helical stretch in the final peptide structures. α-Helix to π-bulge transitions have already been reported in the X-ray structure of the *Penicillium vitale* catalase (*25*), as well as in molecular dynamic simulations for the *c-erbB-2* transmembrane domain (*8*). This type of α-helix distortion has been described to be sequence-dependent and primarily caused by consecutive valine residues. This is indeed what we observe here where the π-bulge appears for the four consecutive residues $V^{24}-V^{27}$. It is interesting to compare our structure to that found earlier by Gullick and co-workers on a shorter version of the TM *neu* peptide (*10*). In that work, an α-helix is also found for the 18-residue-long peptide, which corresponds to residues 4−21 of Neu_{TM35} with Ser substitutions at positions 10, 18, and 21. Unfortunately, the peptide was designed too short to see the π-bulge detected in our work. It has been put forward that increased flexibility could be one consequence

of this π-bulge, inducing modifications in the interactions between helices by changing the interaction faces. This is particularly interesting regarding the fact that *neu/erbB-2* receptor activity is mediated by a dimerization process in which the transmembrane domain is thought to play a major role (*9*). Indeed, the gene known as *neu*, *c-erbB-2*, or *HER-2* is among those most frequently altered in animal and human cancers, especially breast cancers. As already mentioned, a single amino acid substitution within the transmembrane domain of the *neu* protein (Val-664-Glu) converts the *neu* proto-oncogene into a transforming oncogene, *neu**. Of particular interest is the finding that the π-bulge in Neu_{TM35} does not happen in the region where the point mutation (V^{15}) is supposed to occur. Also of interest is the fact that the entire α−π−α helix is 39 Å long, which corresponds to the hydrophobic thickness of most biological membranes. To our knowledge, our data can only be compared to molecular dynamics calculations that describe the TM structure of rat *neu* and ErbB-2 receptors, at the atomic level (*9*). In these simulations performed in vacuo on 25 aa hydrophobic peptides, it appears that there is no concomitant occurrence of π-bulge deformation in the mutation region for wild-type sequences. When the calculations are performed on mutated sequences (V664E for rat *neu* and V659E for *erbB-2*), there are no further occurrences of the helix defect in the mutated region. Although care must be taken in comparing our data to the above results where crude approximations have been made, it is interesting to note that our findings also indicate, and this is to our knowledge the first experimental evidence, that the deformation is not located where the mutation could occur. This suggests that not only point mutations but also intramolecular helicity modulations have to be taken into account in the understanding of the dimerization process. It must be mentioned here that preliminary results by CD spectroscopy did not reveal conformational differences between the wild-type Neu_{TM35} and the mutant Neu_{TM35}* peptide, equally realized by solid-phase synthesis (manuscript in preparation). NMR investigation is under way to figure out if this conformational particularity, the α-helix to π-bulge helix modulation, is maintained in the mutated peptide.

The circular dichroism studies demonstrate that the secondary structure of Neu_{TM35} is essentially the same in TFE, in SDS micelles, and in phospholipid model membranes. The latter are in the form of bicelles, i.e., stable small discoidal objects of 40 Å thickness and of 400−600 Å diameter, whose physicochemical properties have already been well described (*13*, *26*−*29*). Unlike phospholipid liposomes (water dispersions) that diffuse light, the bicelles are almost transparent in circular dichroism conditions, allowing detection of the dichroic signal of a protein potentially embedded in it. As reported herein, CD spectra of 0.5 mol % Neu_{TM35} peptide incorporated into DMPC/DCPC bicelles proved (i) the incorporation of the peptide in the membrane (it would have precipitated in water) and (ii) the maintenance of helical secondary structure elements in this phospholipid environment. Of course circular dichroism cannot provide in great detail the helicity modulations observed by NMR. Although the CD signals in the three media are very close, it cannot be told if the π-bulge observed in TFE solution is retained in the membrane. Of course, organic solvents such as TFE, although they render structure determination by NMR more straightforward, do not provide the same hydrophobic environment as lipids do in biological membranes. We therefore continue NMR investigations on peptide−lipid complexes in our membrane-mimicking system, the DMPC/DCPC bicelles.

In conclusion, we accomplished the first important step in establishing the *neu*/*erbB-2* transmembrane segment's three-dimensional structure in organic solvent. This work settles the basis of structural investigation in a more lipid-like environment. We mastered the incorporation of the peptide in SDS micelles and phospholipid membranes, the bicelles. The peptide's overall helical organization is maintained in these media, as suggested by the corresponding CD spectra. When working with perdeuterated phospholipids, ^{1}H NMR analysis of these original protein−lipid complexes might reveal subtle differences in the molecular structures of Neu_{TM35} and Neu_{TM35}* that could be the key to the very different dimerization behavior of oncogenic *neu**, clarifying the dramatic changes in the receptor activation mechanism.

ACKNOWLEDGMENT

We thank Drs. Serge Geoffre and Philippe Picard (UBS, Bordeaux) for help in solid-phase synthesis and debugging in the GIFA, XEASY, and DYANA programs. Dr. Michel Laguerre (IECB, Bordeaux) is thanked for enlightening explanations on molecular mechanics simulations with the Insight package. Prof. Jean-Yves Lallemand (DCSO, Ecole Polytechnique) is thanked for providing measuring time on the 600 MHz machine at the Ecole Polytechnique and for stimulating discussions.

SUPPORTING INFORMATION AVAILABLE

A table of proton chemical shifts (ppm) of Neu_{TM35} peptide in 100% TFE at 27 °C (2 pages). This material is available free of charge via the Internet at http://pubs.acs.org.

REFERENCES

1. Cao, H., Bangalore, L., Bormann, B. J., and Stern, D. F. (1992) *EMBO J. 11*, 923−932.
2. Chen, L. I., Webster, M. K., Meyer, A. N., and Donoghue, D. J. (1997) *J. Cell. Biol. 137*, 619−631.
3. Smith, S. O., Smith, C. S., and Bormann, B. J. (1996) *Nat. Struct. Biol. 3*, 252−258.
4. Weiner, D. B., Liu, J., Cohen, J. A., Williams, W. V., and Greene, M. I. (1989) *Nature 339*, 230−231.
5. Longo, N., Shuster, R. C., Griffin, L. D., Langley, S. D., and Elsas, L. J. (1992) *J. Biol. Chem. 267*, 12416−12419.
6. Shiang, R., Thompson, L. M., Zhu, Y. Z., Church, D. M., Fielder, T. J., Bocian, M., Winokur, S. T., and Wasmuth, J. J. (1994) *Cell 78*, 335−342.
7. Brandt-Rauf, P. W., Rackovsky, S., and Pincus, M. R. (1990) *Proc. Natl. Acad. Sci. U.S.A. 87*, 8660−8664.
8. Duneau, J. P., Genest, D., and Genest, M. (1996) *J. Biomol. Struct. Dyn. 5*, 753−769.
9. Sajot, N., and Genest, M. (2000) *Eur. Biophys. J. 28*, 648−662.
10. Gullick, W. J., Bottomley, A. C., Lofts, F. J., Doak, D. G., Mulvey, D., Newman, R., Crumpton, M. J., Sternberg, M. J. E., and Campbell, I. D. (1992) *EMBO J. 11*, 43−48.
11. Goetz, M., Rusconi, F., Belghazi, M., Schmitter, J. M., and Dufourc, E. J. (2000) *J. Chromatogr. B 737*, 55−61.
12. Goetz, M., Schmitter, J. M., Geoffre, S., and Dufourc, E. J. (1999) *J. Pept. Sci. 5*, 245−250.
13. Raffard, G., Steinbruckner, S., Arnold, A., Davis, J. H., and Dufourc, E. J. (2000) *Langmuir 16*, 7655−7662.

14. Marion, D., and Wuthrich, K. (1983) *Biochem. Biophys. Res. Commun. 113*, 967−974.
15. Malliavin, T., Pons, J. L., and Delsuc, M. A. (1996) *J. Biomol. NMR 8*, 445−452.
16. Malliavin, T., Pons, J. L., and Delsuc, M. A. (1998) *Bioinformatics 14*, 624−631.
17. Eccles, C., Güntert, P., Billeter, M., and Wütrich, K. (1991) *J. Biomol. NMR 1*, 111−130.
18. Güntert, P., Mumenthaler, C., and Wütrich, K. (1997) *J. Mol. Biol. 273*, 283−298.
19. Manavalan, P., and Johnson, W. C. J. (1987) *Anal. Biochem. 167*, 76−85.
20. Sourgen, F., Maroun, R. G., Frère, V., Bouziane, M., Auclair, C., Troalen, F., and Fermandjian, S. (1996) *Eur. J. Biochem. 240*, 765−773.
21. Lau, S. Y., Taneja, A. K., and Hodges, R. S. (1984) *J. Biol. Chem. 259*, 13253−13261.
22. Cooper, T. M., and Woody, R. W. (1990) *Biopolymers 30*, 657−676.
23. Wüthrich, K. (1986) *NMR of Proteins and Nucleic Acids*, John Wiley, New York.
24. Jones, D. H., Barber, K. R., and Grant, C. W. M. (1998) *Biochim. Biophys. Acta 1371*, 199−212.
25. Vainshtein, B. K., Melik-Adamyan, W. R., Barynin, V. V., Vagin, A. A., Grebenko, A. I., Borisov, V. V., Bartels, K. S., Fita, I., and Rossmann, M. G. (1986) *J. Mol. Biol. 188*, 49−61.
26. Vold, R. R., and Prosser, S. R. (1996) *J. Magn. Reson., Ser. B 113*, 267−271.
27. Sanders, C. R., and Prosser, R. S. (1998) *Structure 6*, 1227−1234.
28. Bian, J., and Roberts, M. F. (1990) *Biochemistry 29*, 7928−7935.
29. Gabriel, E. N., and Roberts, M. F. (1986) *Biochemistry 25*, 2812−2821.

BI0027938